Nonlocal properties of a multidomain magnetic configuration

A. Vanhaverbeke,* O. Klein, and M. Viret
Service de Physique de l'Etat condensé, CEA Saclay, DSM/IRAMIS/SPEC, URA CNRS 2464, 91191 Gif-sur-Yvette, France

J. Ben Youssef
Laboratoire de Magnétisme de Bretagne (UMR 6165 CNRS), Université de Bretagne Occidentale, 6 Avenue Le Gorgeu, 29285 Brest Cedex, France

(Received 22 August 2008; revised manuscript received 31 August 2009; published 12 November 2009)

We study the nonlocal properties of the magnetic multidomain configuration of a soft ferrimagnetic iron garnet using an original combination of two local probe techniques. The domain pattern of the garnet, which has a strong perpendicular anisotropy, consists of a maze of alternating up and down domains that are several micrometers wide. The magnetic tip of a scanning force microscope is used to locally excite this configuration. The resulting long-range perturbation is measured by a static nickel Hall cross deposited on top of the garnet, which is used as another local (magnetoresistive) sensor. It is found that punctually perturbing a domain-wall affects the magnetic configuration several domains away on distances well over the 5 μm range.

DOI: 10.1103/PhysRevB.80.184414 PACS number(s): 75.70.Kw, 75.50.Gg, 73.43.Qt

The forced displacement of magnetic domains wall inside a ferromagnetic thin-film has been the object of intense research for many years.[1] The discovery of current-induced domain-wall motion[2–4] and its potential applications for spintronics[5,6] have boosted studies on domain-wall displacement, where this inhomogeneity of the magnetic configuration might provide an advantageous replacement for the multilayer heterogeneous structures. Most studies have focused on the *individual* displacement of domain walls and the *collective* aspect of the problem within the entire multidomain magnetic structure has been ignored. Experimentally, there are very few tools[7] capable of measuring precisely nonlocal effects in the micrometer range, which is the relevant length scale. We present here an original combination of two local probe techniques to study the response to a punctual perturbation several micrometers away. The tip of a magnetic force microscope (MFM) is used to locally perturb the magnetic domains of a *maze* pattern[7] inside a perpendicular iron garnet film. This large coupling regime is at the opposite end of the normal use of MFM, where good imaging conditions usually require decreasing the tip or sample interaction[8] to allow imaging of unperturbed domains. The tip produces an additional magnetic field which favors magnetic domains that are aligned with the tip direction. This local effect is in contrast to a global evolution under a homogeneous additional magnetic field.[9,10] The long-range effect of this perturbation on the domain structure is measured at another position by a magnetoresistive measurement, here a submicrometer nickel Hall cross, deposited on top of the sample. These unique nonlocal measurements allow us to determine the range of the domains perturbation by the tip. Using micromagnetic simulations, we can also illustrate the domains perturbation mechanism.

The investigated magnetic system is a 5.4-μm-thick layer of $(SmLuBi)_3Fe_5O_{12}$ grown by liquid-phase deposition on a gadolinum gallium garnet (GGG) substrate. This very soft ferrimagnetic material with perpendicular anisotropy forms typical maze structure domains, whose relative widths and periodicity can be controlled with a perpendicular magnetic field similarly to what was demonstrated in FePd samples.[9] The magnetic properties of the iron garnet were measured with a vibrating sample magnetometer and are summarized in Table I. These values were further validated by comparing the ratio of minority or majority domain sizes obtained with the Kooy-Entz model[11] to MFM images measured at various perpendicular fields.

Our experimental setup is based on a custom magnetic force microscope, which can be inserted between the polar pieces of a 1.6 T electromagnet. We use a commercial magnetic tip with CoCr coverage of high magnetic moment and whose coercive field was measured to be 10 mT. MFM measurements were made using the so-called *interleave* mode: during a first scan, the topography of the surface is recorded keeping the cantilever amplitude constant and during the second scan, the tip was lifted by 50 nm to measure the magnetic force signal with minimal perturbation. All the data presented here correspond to the lifted scan.

The other local probe was a Hall cross patterned by electron-beam lithography and argon-ion etching in a 10-nm-thick Ni layer deposited on top of the insulating iron garnet film. Galvanomagnetic measurements were carried out in real time with a lock-in technique using a time constant of 30 ms and an injected current frequency of 270 Hz. A typical sensitivity of 1% of the planar Hall signal amplitude was achieved. The measurements were made *in situ*, which al-

TABLE I. Magnetic parameters of the ferrimagnetic iron garnet and ferromagnetic nickel layers.

Magnetic garnet: $(SmLuBi)_3Fe_5O_{12}$	
Exchange stiffness	3.5×10^{-12} J/m
Saturation magnetization	140×10^{3} A/m
Anisotropy energy	2.7×10^{4} J/m^3
Nickel thin film	
EHA resistivity	-2×10^{-9} Ω/m
$\rho_{\parallel}-\rho_{\perp}$	$1.7\pm0.1\times10^{-9}$ Ω/m

lows correlating the lateral position of the MFM tip and any change in the magnetoresistive signal. A constant shift of 100 ms between the MFM and Hall voltage signals due to delays and time constant of the resistivity data acquisition was corrected by slightly shifting one image respective to the other. Slow tip scanning, typically 5 s per line, is well adapted to get a good signal-to-noise ratio for the magnetoresistive measurements and at the same time limiting the lock-in amplifier time response.

Nickel transport properties were studied in identical Hall crosses patterned on a nonmagnetic GGG substrate; we could derive from those measurements the magnetoresistive parameters for the nickel layer given in Table I. We considered for simplicity that the magnetization in the 200×200 nm^2 area in the nickel Hall cross can be represented by a macrospin with free parameters θ, the in-plane rotation angle, and m_z, the perpendicular component of the normalized magnetization. Neglecting the ordinary Hall effect, the Hall resistance is then given by Eq. (1) (Ref. 12)

$$R_H = \frac{E_H}{j} = \frac{[\rho_\parallel - \rho_\perp]}{2}(1-m_z^2)\sin 2\theta + \rho_{HA} m_z. \qquad (1)$$

The first part of the right-hand side of the equation is called the planar Hall effect; the second part is the extraordinary Hall effect. We checked with micromagnetic simulations[13] that, due to the strong vertical demagnetizing factor in the cross, the nickel magnetization is mainly sensitive to planar fields, so the planar Hall effect will be the main contributor to the magnetoresistive signal.

As we scan the MFM tip over the surface of the sample, two different effects are visible in the tip-position-dependent Hall signal:

Local effect. The magnetic tip stray field directly influences the magnetization in the nickel Hall cross. This is similar to experiments where the normal Hall effect in a semiconductor Hall cross is used to characterize the MFM tip stray field.[14] Figure 1(a) (Ref. 15) illustrates this effect when a large magnetic field (200 mT) is applied to magnetically saturate the ferrimagnetic garnet. We observe a bipolar change of the Hall resistance when the tip is close to the Hall cross. From symmetry considerations, we can deduce that this bipolar effect comes from an in-plane rotation induced by the in-plane component of the tip stray field and measured by a change in the planar Hall resistance. The Hall effect changes when the tip is less than 1.6 μm away from the cross which gives the range of the tip stray field. Using Fig. 1(a), we could determine the unperturbated direction of the nickel magnetization in the Hall cross: its angle is given by the antisymmetry axis of the dark-clear pattern and its direction is deduced from the tip stray-field polarity as explained in Fig. 1(c); when the tip is in position 1 (respectively, 2), its stray field makes the magnetization rotate anticlockwise (respectively, clockwise) which increases (respectively, decreases) the planar Hall resistance.

Nonlocal effect. The tip stray field influences the ferrimagnetic garnet magnetic domains, in particular when the tip is close to a domain wall. The nickel probe then measures a change in the domains stray field, mainly its in-plane component. Such a nonlocal measurement, where we excite the magnetic system and probe the effect at a different position, is presented in Fig. 2 where we have positioned a single minority domain close to the Hall cross by applying a perpendicular magnetic field of 130 mT.

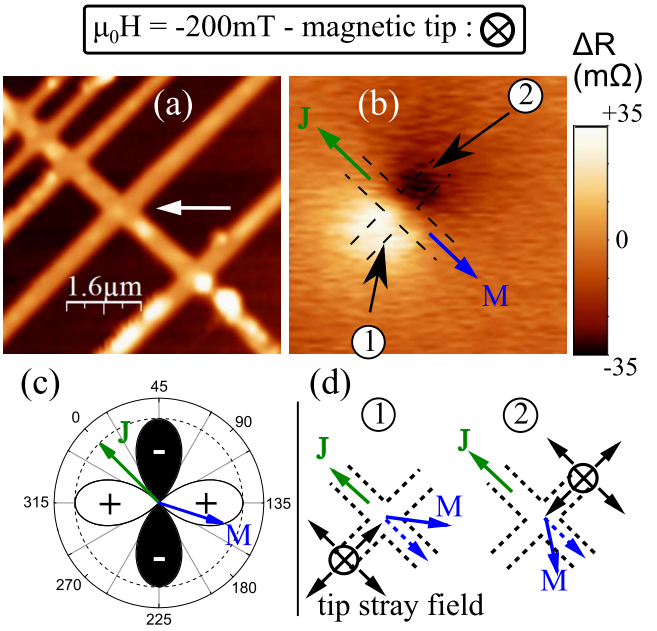

FIG. 1. (Color online) Local influence of the MFM tip stray field on the magnetization at the center of a submicrometer-size nickel cross. The tip is magnetized toward the sample by a large (200 mT) perpendicular field which also saturates the garnet underneath. (a) Atomic force microscopy (AFM) topography image. The nickel cross where the Hall signal is measured is indicated by a white arrow. (b) Hall effect variation with tip position. The position of the Hall cross is indicated with dashed lines. (c) Schematics of the amplitude of the planar Hall effect as a function of the angle between the current **J** and the magnetization **M**. (d) Effect of the planar component of tip stray field (black arrows) on the cross magnetization (blue arrow); the continuous (respectively, dashed) blue arrow shows the perturbed (respectively, unperturbed) magnetization direction in the nickel Hall cross for two different tip positions.

The dark MFM contrast associated to the tip passing above the minority domain in Fig. 2(a) is correlated with a change in the Hall signal marked by a dashed line in Fig. 2(b). Since this effect is visible for different scan lines, it must correspond to a reproducible displacement of the magnetic domains in the iron garnet induced by the tip as it passes over a minority domain. Only during the scan of the tip in the opposite direction do the domains recover their initial position. It is worth noticing that the effect is reproducible for very different crossing positions, showing that local pinning plays a weak role compared to a rearrangement of the domain structure and that the domains present a longitudinal rigidity over several micrometers.

To determine whether this effect modifies the planar or the perpendicular component of the magnetization in the nickel Hall cross, we permuted the current and voltage leads in the Hall cross and repeated the scan: polarity from the planar Hall effect is then reversed, whereas the anomalous Hall effect is kept the same. By subtracting these two Hall

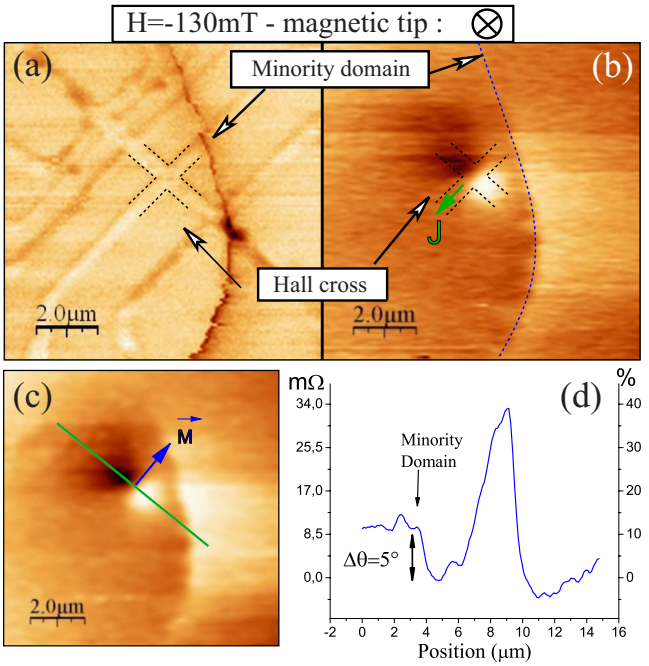

FIG. 2. (Color online) Double magnetic imaging with one minority domain of the garnet close to the nickel Hall cross. (a) MFM image. The minority domain can be seen as a black narrow stripe. The contrast associated to the nickel structure is an artifact due to the topography. (b) Hall effect in the cross (represented by dashed lines). The local effect of the tip stray field and the interaction with the minority domain are both visible. (c) Planar Hall effect resulting from the subtraction of the image (b) and the equivalent image after rotating current injection and voltage measurement by 90°. (d) Profile on (c) (green line) showing the change in planar Hall effect and the corresponding angle θ. Fast scan of the tip is from right to left.

maps [Fig. 2(c)], we can establish that the planar Hall effect is the main component of the signal for both local and nonlocal effects. Using Eq. (1), we can also determine the nonlocal tip-induced rotation in the Hall cross to be about 8°. Knowing the orientation of the nickel magnetization and of the garnet stray field, we can deduce from Fig. 2(c) that the minority domain is pushed away from the Hall cross when the tip is scanned above from right to left. Consequently, we named this phenomenon the *domain backlash effect*.

A clear understanding of the interaction between MFM tip and the domains in the garnet was obtained using micromagnetic simulations. We used the OOMMF framework[13] with an extension for periodic boundary conditions.[16] The modeled section of the sample is 960×96 nm^2 and the period is 360 nm along the direction of the domain walls, with a cell size of $6\times6\times6$ nm^3. We used the garnet properties given in Table I. The thickness, and as a result, the domain sizes were reduced so as to remain within a reasonable simulation size. Thus, unfortunately, the system modeled is not the real measured one and the results are not to be taken quantitatively. Nevertheless, our goal here is to show that the backlash effect is quite a general feature in these magnetic multidomain states. The magnetic tip stray field is simulated using the field produced by a magnetic monopole, following the relation

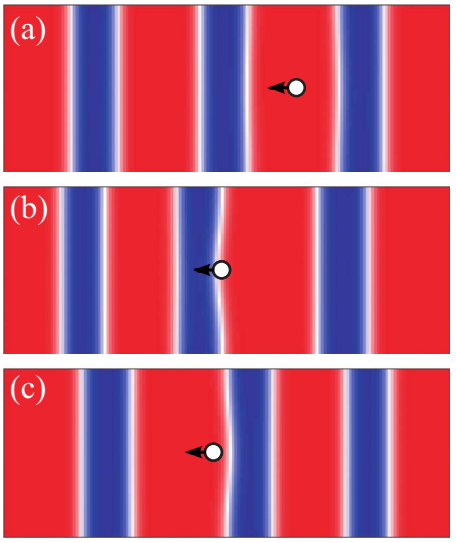

FIG. 3. (Color online) Micromagnetic simulations showing the domains backlash effect induced by the magnetic tip in the strong-interaction regime. A homogeneous magnetic field $\mu_0 H=25$ mT is applied; only the perpendicular magnetization value in the top surface of the garnet is shown. The magnetic monopole ($q=-1.0\times10^{-9}$ A m) is scanned 50 nm above the surface of the 96-nm-thick garnet. (a) As the monopole is above a majority domain (red), the domains are close to equilibrium.(b) Getting close to a minority domain (blue), the monopole drags forth the domain walls: the majority domain below the monopole gets larger. (c) After crossing, the monopole pushes backward the minority domain and the next majority domain gets larger.

$$\vec{H}(\vec{r}) = \frac{q}{r^2}\vec{e}_r,$$

where $\vec{e}_r$ is the unitary vector pointing from the monopole to the position $\vec{r}$. The monopole strength $q=-1.0\times10^{-9}$ A m and height above the surface=50 nm were chosen so as to be compatible with the measured stray field of a similar tip.[17] The position of the monopole is changed by step of 18 nm perpendicular to the domain walls and after each step, the garnet domains are relaxed toward the minimum of energy. We can thus simulate the quasistatic response of the domains to the tip excitation during the MFM scan.

Figure 3(a) shows the magnetic domains at equilibrium with an applied magnetic field of +25 mT, defining majority domains (shown as red) and minority domains (shown as blue). The monopole is located above a majority domain so its positive field does not modify the magnetization. When the tip gets close to a minority domain, its stray field extends the size of the majority domain and pushes forward the minority one. These effects get bigger as the tip comes closer to the center of the minority domain at equilibrium [Fig. 3(b)]. At some point, it becomes energetically favorable for the minority domain to jump back behind the magnetic monopole as shown in Fig. 3(c). The resulting effect is that the minority domain is pushed backward as the tip is scanned above it as was observed in the experiments.

The simulation also explains a scan-direction-dependent feature on MFM images of the garnet in the high interaction

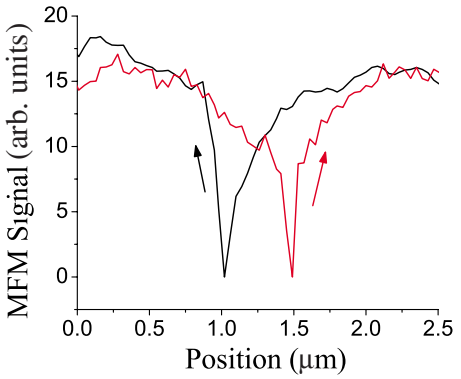

FIG. 4. (Color online) Magnetic force microscopy profiles above the garnet minority domain in the high interaction regime for both scan directions. A perpendicular field of $\mu_0 H = -120$ mT is applied. A larger (respectively, smaller) value of the MFM signal corresponds to a more (respectively, less) attractive interaction between the tip and the sample.

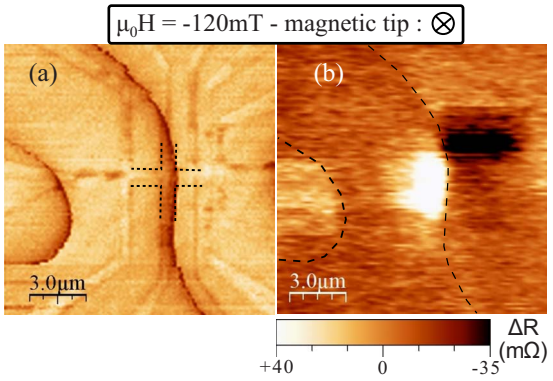

FIG. 5. (Color online) Double imaging of the system including several minority domains. Fast scan of the tip is from left to right. (a) MFM image with the Hall cross position indicated by black dashed lines. The dark contrast lines correspond to the two minority domains artificially narrowed by the tip dragging the domain wall and inducing the backlash effect. (b) Hall voltage sensed in the nanostructured cross as a function of the tip position. The backlash positions given by the dark domains of (a) are reported in dashed lines. A brighter area at the left of the left dashed line is visible, even though the sensing cross is over one period of minority or majority domains away. This is due to the backlash of the left minority domain which induces a rotation of the magnetization in the cross of about 5°.

regime. Figure 4 shows the MFM signal in back and forth line scans perpendicular to a minority domain. When the tip gets closer to the minority domain, there is a progressive decrease of the MFM signal before the backlash itself. Then, the signal increases abruptly. We interpret this effect as a reduction of the stray field sensed by the tip when it extends locally the majority domain into the minority domain as shown on Fig. 3(b). After the backlash, the minority domain is repelled far away from the tip, leading to a sharp increase of the MFM signal at that point.

Our micromagnetic simulations also show that the minority domain backlash modifies the domain structures over several periods of domains. We checked that this also happens in our sample by scanning the MFM tip over a larger area and with a reduced magnetic field, $\mu_0 H = 120$ mT, to observe the domain backlash effect on several parallel minority domains. The resulting MFM imaging is shown in Fig. 5(a) where the dark lines are the minority domains artificially narrowed because of the interaction between the tip and the sample. The Hall cross is drawn in with dashed lines. Figure 5(b) shows the evolution of the Hall voltage as the tip is scanned over the sample with the two minority domains marked by black dashed lines. One of the minority domains is located very close to the Hall cross and as a result, we measure a large change of the Hall effect when the tip is scanned over it, as visible in Fig. 5(b). More importantly, we also see that a change in the Hall effect, corresponding to a 5° rotation of the magnetization in the Hall cross, occurs for the tip crossing the next minority domain on the left. This demonstrates that on a large scale of at least 5 μm, the backlash effect is transmitted from one minority domain to the next, in qualitative agreement with our micromagnetic calculations. The backlash effect is transmitted over several domains periods due to an elasticity of the domain pattern which tries to keep each majority or minority domain relative widths constant when one domain position is changed so as to minimize the demagnetization energy.

Finally, understanding the principle of the domain backlash effect, we could estimate the domain displacement induced by the tip in Fig. 5. We make the assumption that the minority domain is just in front of the tip before the backlash occurs and that the width change of the minority domains is negligible. The difference in the backlash position for the two opposite scan directions was measured to be 500 nm and the Kooy-Enz model gives a minority domain width of 800 nm for an applied field of 120 mT. Thus the minority domain is displaced by 1.3 μm during the back-and-forth scans of the tip above it.

In summary, we have studied the nonlocal response of a magnetic domain structures to a local excitation with an original two-local-probe technique. The passing of an MFM tip above a minority domain triggers a collective domain backlash which can be measured over several micrometers along the domain walls and over several periods of domains by a magnetoresistive measurement.

*antoine.vanhaverbeke@gmail.com

[1] A. P. Malozemoff and J. C. Slonczewski, *Magnetic Domain Walls in Bubble Materials* (Academic Press, New York, 1979).
[2] A. Yamaguchi, T. Ono, S. Nasu, K. Miyake, K. Mibu, and T. Shinjo, Phys. Rev. Lett. **92**, 077205 (2004).
[3] L. Berger, J. Appl. Phys. **55**, 1954 (1984).
[4] S. Zhang and Z. Li, Phys. Rev. Lett. **93**, 127204 (2004).
[5] S. S. P. Parkin, M. Hayashi, and L. Thomas, Science **320**, 190 (2008).
[6] D. A. Allwood, G. Xiong, C. C. Faulkner, D. Atkinson, D. Petit,

and R. P. Cowburn, Science **309**, 1688 (2005).
[7] A. Hubert and R. Schäffer, *Magnetic Domains: The Analysis of Magnetic Microstructures* (Springer, New York, 1998), p.84; A. Thiaville, L. Belliard, and J. Miltat, Proceedings of the Conference Scanning Microscopy International, Chicago, 1997 (unpublished).
[8] J. M. Garcia, A. Thiaville, J. Miltat, K. J. Kirk, J. N. Chapman, and F. Alouges, Appl. Phys. Lett. **79**, 656 (2001).
[9] O. Klein, Y. Samson, A. Marty, S. Guillous, M. Viret, C. Fermon, and H. Alloul, J. Appl. Phys. **89**, 6781 (2001).
[10] U. Ebels, L. Buda, K. Ounadjela, and P. E. Wigen, Phys. Rev. B **63**, 174437 (2001).
[11] C. Kooy and U. Enz, Philips Res. Rep. **15**, 7 (1960).
[12] R. C. O'Handley, *Modern Magnetic Materials—Principles and Applications* (Wiley InterScience, New York, 2000).
[13] M. J. Donahue and D. G. Porter, National Institute of Standards and Technology Technical Report No. 6376, 1999 (unpublished).
[14] A. Thiaville, L. Belliard, D. Majer, E. Zeldov, and J. Miltat, J. Appl. Phys. **82**, 3182 (1997).
[15] We used the WSXM software for scanning probe images processing. See I. Horcas, R. Fernández, J. M. Gómez-Rodríguez, J. Colchero, J. Gómez-Herrero, and A. M. Baro, Rev. Sci. Instrum. **78**, 013705 (2007).
[16] K. M. Lebecki, PBC Module for OOMMF. See http://info.ifpan.edu.pl/lebecki/pbc.
[17] S. McVitie, R. P. Ferrier, J. Scott, G. S. White, and A. Gallagher, J. Appl. Phys. **89**, 3656 (2001).